Scintigraphy and Single-Photon Emission Computed Tomography

19

Kenichi Nakajima, Anri Inaki, Seigo Kinuya,
Takashi Wada, and Mitsuhiro Kawano

19.1 Whole-Body Evaluation with ^{67}Ga Scintigraphy

^{67}Ga is a metal ion that belongs to the third group of the periodic table. This ion is transported to target organs after binding with transferrin in the blood. ^{67}Ga is a classic agent in the field of nuclear medicine and has been employed widely in the investigation of malignant and inflammatory processes. SPECT scanning is particularly useful in lymphoma, undifferentiated cancer, and malignant melanoma, but also accumulates avidly in nonmalignant inflammatory conditions such as sarcoidosis, infections, and abscesses.

^{67}Ga shows diffuse accumulation in interstitial diseases of the lung and kidney when the process is active. With the recent widespread availability of ^{18}F-fluorodeoxyglucose/positron emission tomography (FDG-PET), the use of ^{67}Ga to diagnose cancer and metastases has declined. ^{67}Ga is still used frequently to search for systemic involvement, however, because its accumulation correlates well with parenchymal or interstitial inflammatory changes.

^{67}Ga accumulates physiologically in the nasopharynx, lacrimal gland, parotid gland, bowel excretion, and liver. When evaluating the degree of accumulation at these sites, the first step of interpretation is to judge whether it is physiological or pathologic. In addition, the degrees of accumulation in the bone marrow, pulmonary hila (usually symmetric), and breasts show individual variations, which must be taken into consideration.

In general, abnormalities related to autoimmune dysfunction include systemic lymph node involvement, interstitial pneumonia, pleuritis, pericarditis, pancreatitis, inflammatory changes of the hepatobiliary tree, retroperitoneal fibrosis, sialadenitis, interstitial nephritis, arthritis, and thyroiditis. All of these organs and tissues are known to be affected by IgG4-related disease (IgG4-RD). An advantage of whole-body ^{67}Ga imaging is that this imaging approach can identify abnormal regions throughout the body with just one study. ^{67}Ga scintigraphy is also performed sometimes to monitor changes in the degree of accumulation as an index of the effect of therapy. The usefulness of whole-body ^{67}Ga scintigraphy or SPECT has been reported not only in the pancreas as related to autoimmune pancreatitis (AIP) but also in extrapancreatic lesions including those in the lung, lymph nodes, and kidney [1–7]. In Mikulicz's disease, abnormal accumulations have also been detected in the lacrimal gland, salivary gland, and kidney [8].

19.1.1 Case 1: ^{67}Ga Accumulation in the Salivary Glands and Kidneys

A woman in her late 70s sought medical attention because of bilateral submandibular gland swelling. The etiology of her complaint remained unclear despite a salivary gland biopsy. During the work-up of another condition, however, the presence of renal dysfunction became clear when an elevated serum creatinine value, proteinuria, and hematuria were detected. Hypocomplementemia, hypergammaglobulinemia, and elevated IgG4 concentration (486 mg/dL) were also noted. On renal biopsy, a marked inflammatory infiltrate within the interstitium was found, and the diagnosis of IgG4-RD was proposed.

K. Nakajima (✉) • A. Inaki • S. Kinuya
Department of Nuclear Medicine, Kanazawa University,
Takara-machi, Kanazawa 920-8641, Japan
e-mail: nakajima@med.kanazawa-u.ac.jp

T. Wada
Division of Nephrology, Department of Laboratory Medicine,
Kanazawa University, Takara-machi, Kanazawa 920-8641, Japan

M. Kawano
Division of Rheumatology, Kanazawa University Hospital,
Takara-machi, Kanazawa 920-8641, Japan
e-mail: sk33166@gmail.com

H. Umehara et al. (eds.), *IgG4-Related Disease*, DOI 10.1007/978-4-431-54228-5_19,

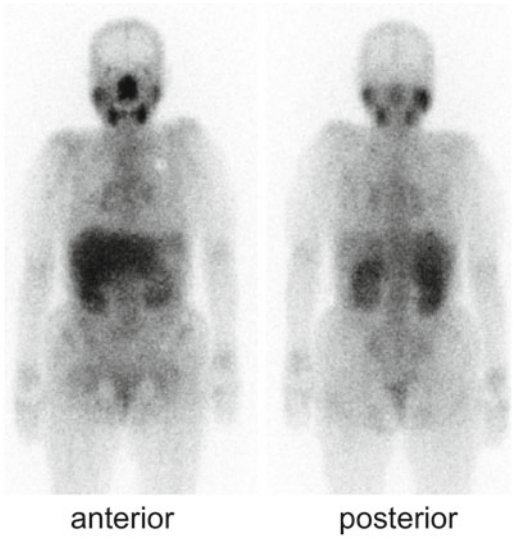

Fig. 19.1 Accumulation in the salivary glands and kidneys on whole-body ^{67}Ga scintigraphy (anterior and posterior views)

On ^{67}Ga scintigraphy, high accumulation was found in the bilateral parotid and submandibular glands. Symmetrical high accumulation was observed in the bilateral kidneys (Fig. 19.1).

19.1.2 Case 2: IgG4-RD Lesions of the Pancreas, Lung, and Periaortic Tissues

A man in his early 60s presented with abdominal pain and was diagnosed with type 1 AIP. He subsequently became aware of diplopia and a magnetic resonance imaging (MRI) study revealed pituitary gland swelling. On biopsy, a lymphoplasmacytic infiltrate enriched with IgG4-positive plasma cells was found, and IgG4-RD was diagnosed.

Whole-body SPECT scanning was performed. Abnormal ^{67}Ga accumulation was observed in the mediastinum (including the pulmonary hila), the right lower lung field, and the midline of the abdomen on both the whole-body image (a) and the abdominal SPECT coronal section (b). Based on the CT coronal sections (c), SPECT-CT software-generated fusion images were created (d). A soft tissue density shadow was found extending from the abdominal aorta to the common iliac artery (Fig. 19.2).

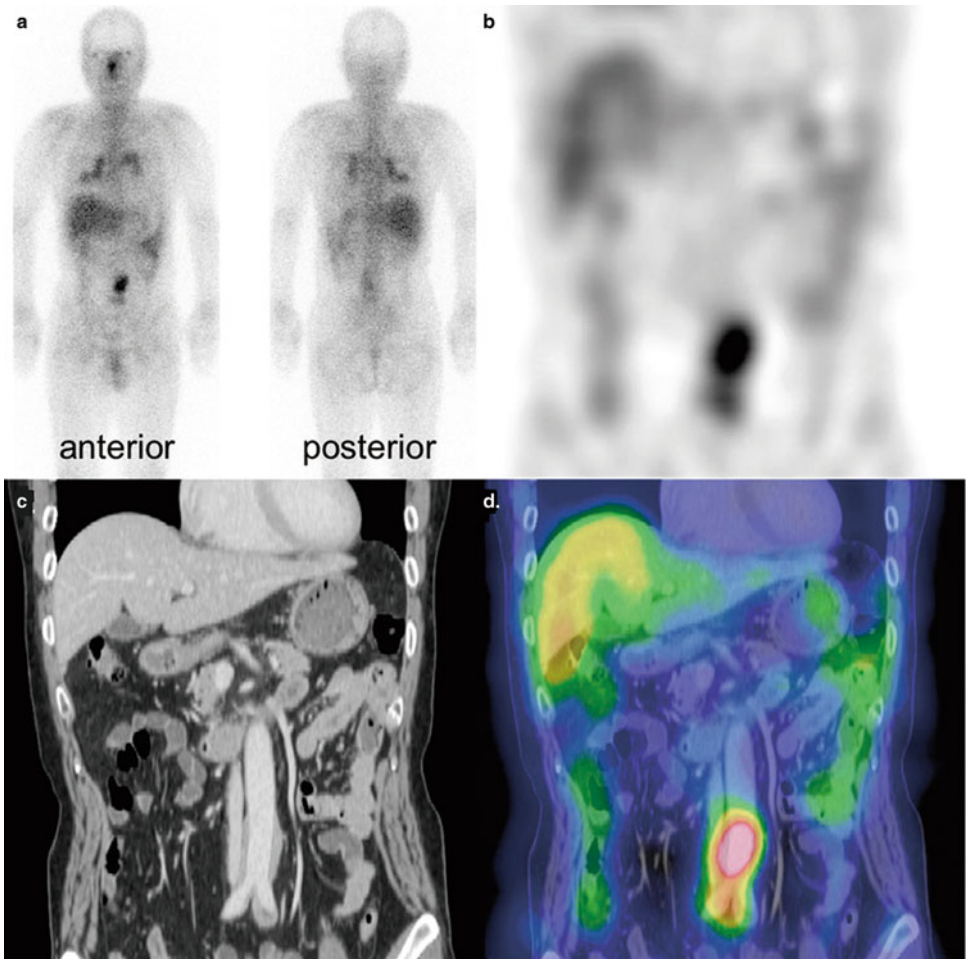

Fig. 19.2 Detection of pancreatic, pulmonary, and periaortic lesions by whole-body ^{67}Ga scintigraphy (**a**) and SPECT (**b**–**d**)

19.1.3 Case 3: IgG4-Related Lesions of the Pancreas

A man in his late 70s presented with intermittent left abdominal pain. On abdominal US and CT, pancreatic swelling and irregular stenosis of the main pancreatic duct were noted, and laboratory examinations showed an elevated serum IgG4 value. On pancreatic biopsy, IgG4-positive lymphoplasmacytic infiltrate was found and IgG4-RD diagnosed.

On whole-body SPECT imaging, ^{67}Ga accumulation was noted at multiple sites within the abdomen (a), but differentiation from accumulation in the digestive tract was difficult. The abdominal SPECT coronal and CT coronal sections (b and c, respectively) were also indeterminate. However, on the SPECT-CT fusion image, the accumulation in the midline was consistent with the marked accumulation seen in the pancreas (d). There was also a horizontal, band-like collection in the transverse colon felt to represent physiological accumulation. However, the area indicated by the thick arrow shows abnormal accumulation in the pancreas (a) (Fig. 19.3).

19.2 Salivary Gland Scintigraphy

Salivary gland scintigraphy is usually performed as a dynamic image data acquisition for 20–45 min after an intravenous injection of ^{99m}Tc pertechnetate. Accumulation in the parotid and submandibular glands and excretory function into the oral cavity after vitamin C administration are evaluated together. As a quantitative analysis, regions of interest are set on four salivary glands and background areas, and time-activity curves are created. Quantitative parameters include degree of accumulation in each gland and washout rate after stimulation by vitamin C. The aims of the examination are to assess salivary gland dysfunction related to IgG4-RD and to evaluate the impact of therapy.

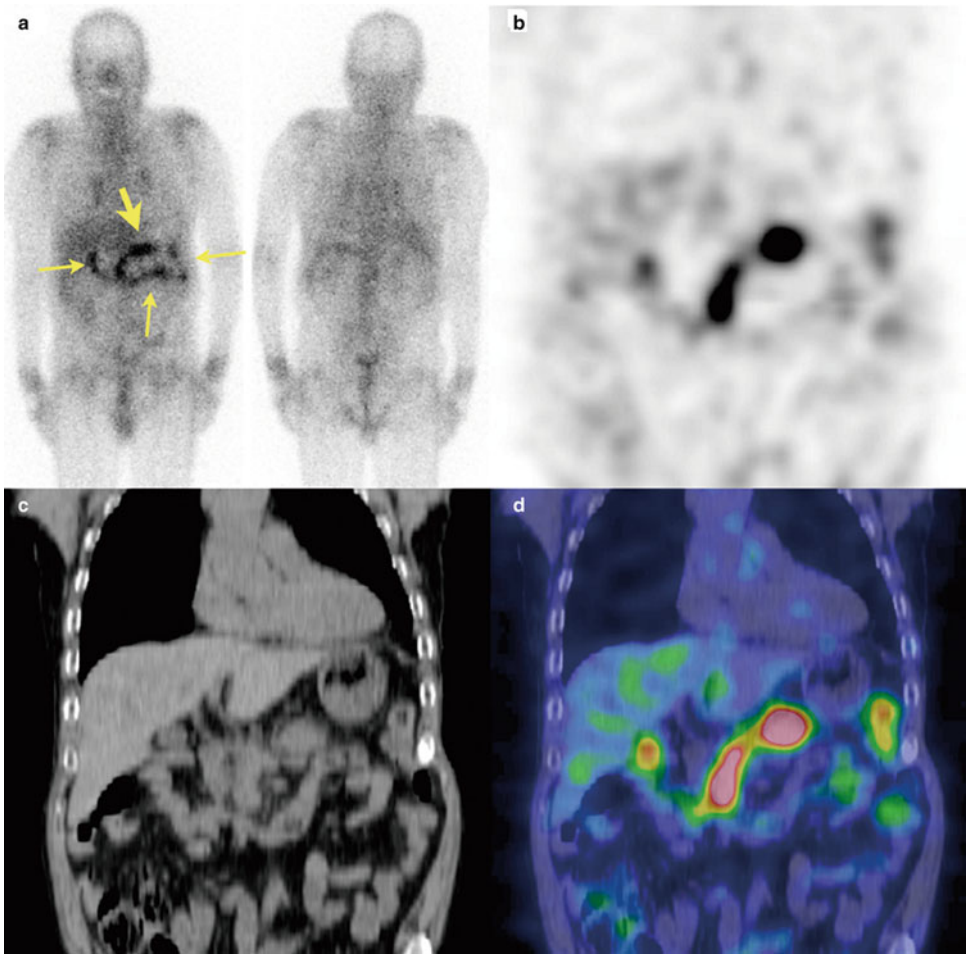

Fig. 19.3 Detection of pancreatic lesions by whole-body ^{67}Ga scintigraphy (**a**) and SPECT (**b–d**). On coronal section fusion image (**d**), clear accumulation in the pancreas is seen

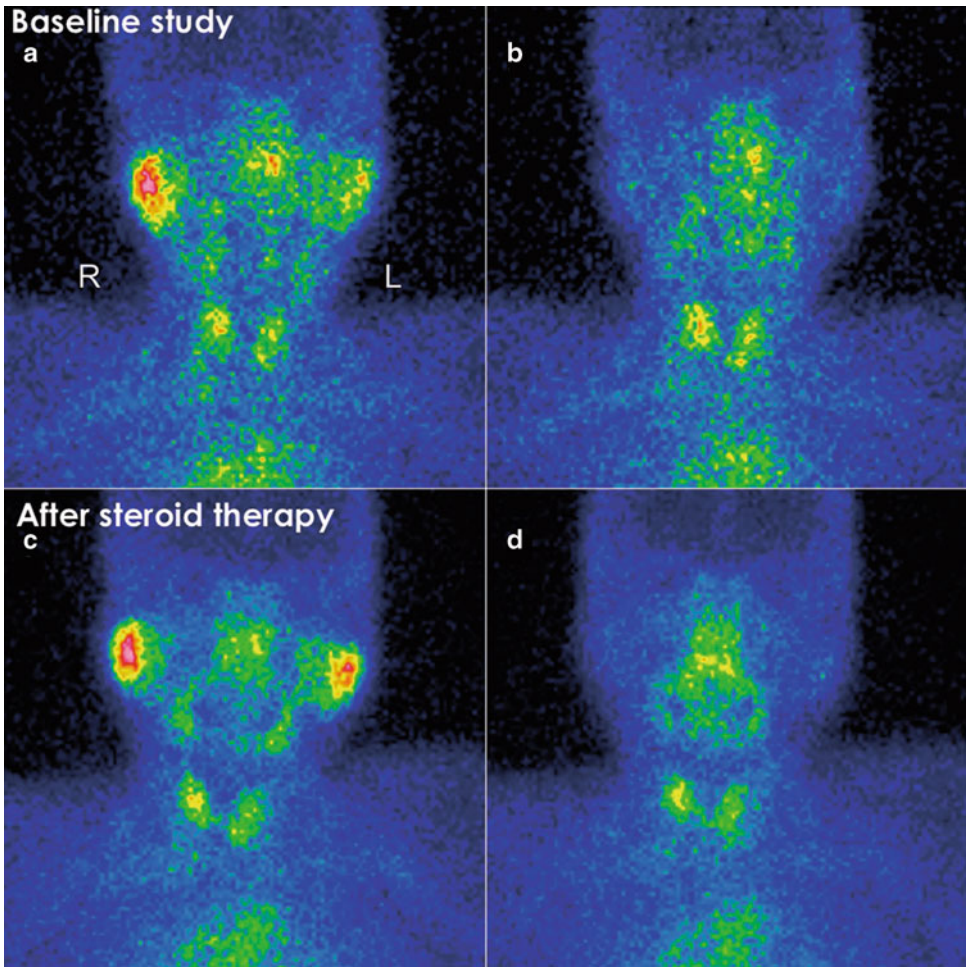

Fig. 19.4 Changes in salivary gland function before and after therapy (**a**, **b**) pre-therapy; (**c**, **d**) post-therapy

Table 19.1 Changes in salivary gland function before and after therapy in case 4

	Submandibular glands	Parotid glands	Submandibular/parotid uptake ratio
Salivary gland uptake/background ratio			
Before therapy	4.05	5.72	0.71
After therapy	5.17	5.95	0.87
Washout rate (%)			
Before therapy	1.9 %	56.3 %	0.03
After therapy	21.7 %	61.9 %	0.35

19.2.1 Case 4: Changes in Salivary Gland Function Before and After Therapy

A woman in her late 70s (the same patient described in Case 1, above) had submandibular gland swelling for 20 years. Two years before presentation an MRI study had shown symmetrical swelling of the lacrimal, parotid, and submandibular glands, and a minor salivary gland biopsy of the lower lip had revealed a lymphoplasmacytic infiltrate that stained positively for IgG4-bearing plasma cells. The serum IgG4 concentration was 696 mg/dL, and anti-SS-A/B antibodies were negative.

The patient was treated with glucocorticoids and scintigraphy was performed before and after this intervention. The upper images in Fig. 19.4 show the findings before therapy, and the lower ones illustrate those following treatment. Before therapy accumulation in the bilateral parotid glands was relatively well preserved, whereas that in the submandibular glands was markedly and heterogeneously decreased (a). Washout after vitamin C administration was also decreased (b). On post-therapy scintigraphy, accumulation in the submandibular glands became clearer (c), and washout was also improved (d) (Fig. 19.4). In a semiquantitative evaluation using the accumulation count, both the washout rate after vitamin C administration and the accumulation in the submandibular glands as compared with the parotid showed clear improvement (Table 19.1).

19.3 Renal Scintigraphy

For the evaluation of renal function, renal dynamic imaging is performed using ^{99m}Tc-diethylene-triamine-pentaacetic acid (DTPA). Renograms are created for each kidney and split glomerular filtration rate is calculated. Renal cortex imaging using ^{99m}Tc-dimercaptosuccin acid (DMSA) is also utilized. Because of limited resolution in ^{99m}Tc-DTPA examination, minor functional abnormalities cannot be detected, but areas with major functional decreases in each kidney can be identified. ^{99m}Tc-DMSA static scintigraphy and SPECT are used to detect renal cortical fibrosis. With regard to renal lesions, ^{67}Ga scintigraphy is performed to assess the inflammatory response [3, 8], while DTPA and DMSA scintigraphies are indicated for the evaluation of function and fibrosis.

19.3.1 Case 5: Renal Cortical Lesions

A man in his early 60s presented 1 year earlier after noticing bilateral submandibular swelling. Bilateral submandibular gland swelling, pancreatic tail lesions, bilateral renal lesions, and lesions around the aorta and right internal iliac artery were demonstrated by contrast-enhanced CT. A renal biopsy was consistent with IgG4-RD. The serum IgG4 concentration was 350 mg/dL.

On DMSA scintigraphy, localized sites of decreased accumulation were found in the upper part of the left kidney and both the upper and lower poles of the right kidney (a, arrows). In the arterial phase of contrast-enhanced dynamic CT, heterogeneous enhancement of the cortex was noted mainly at the same sites (b) (Fig. 19.5).

19.4 Concluding Remarks

In this chapter we presented a number of IgG4-RD cases to outline the various examination methods using single-photon radionuclides that are useful in this context. ^{67}Ga inflammation scintigraphy has frequently been used for whole-body screening for lesions, but the diagnostic accuracy of IgG4-RD as compared with FDG-PET will require additional study. For other functional and static evaluations, a number of other scintigraphic examinations can be also used (Table 19.2). In any case, although scintigraphic evaluation was not specific for IgG4-RD, it provides information on organ function and an index for diagnosis and therapeutic effects. Combined use of SPECT-CT is recommended to confirm functional-anatomical correspondence.

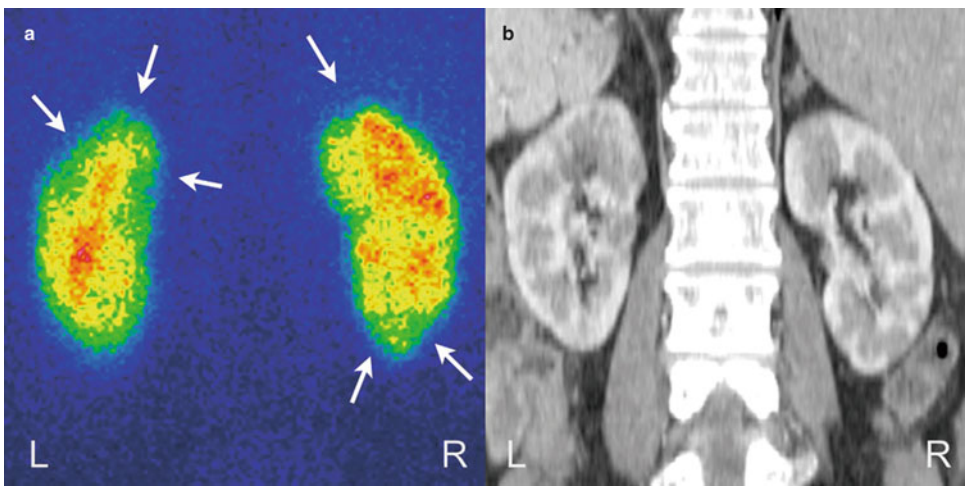

Fig. 19.5 Evaluation of lesions by renal cortex scintigraphy (**a**). To compare the anterior CT images with the posterior images on scintigraphy, left-right inversion of the former was performed (**b**)

Table 19.2 Functional evaluation using single-photon radiopharmaceuticals of organs with possible IgG4 disease involvement

Organ	Scintigraphy	Radiopharmaceutical	Application
Whole body	^{67}Ga scintigraphy, SPECT	^{67}Ga-citrate	Detection of inflammatory lesions and severity (lacrimal glands, salivary glands, lungs, pancreas, kidneys, retroperitoneum, mediastinum, pleura, pericardium, great vessels, intraorbital tissues)
Salivary glands	Salivary gland scintigraphy	^{99m}Tc-pertechnetate	Impaired accumulation and excretion
Liver and bile ducts	Hepatobiliary scintigraphy	^{99m}Tc-PMT	Abnormal excretion due to cholangitis
Kidney	Renal cortical perfusion scintigraphy, renal dynamic study	^{99m}Tc-DMSA, ^{99m}Tc-DTPA	Cortical perfusion defect, abnormality in blood flow and excretion

References

1. Saegusa H, Momose M, Kawa S, Hamano H, Ochi Y, Takayama M, et al. Hilar and pancreatic gallium-67 accumulation is characteristic feature of autoimmune pancreatitis. Pancreas. 2003;27:20–5.
2. Ando N, Yasuda I, Saito M, Moriwaki H. Hilar lymphadenopathy associated with autoimmune pancreatitis. Pancreas. 2006;33:101–2.
3. Saeki T, Nishi S, Ito T, Yamazaki H, Miyamura S, Emura I, et al. Renal lesions in IgG4-related systemic disease. Intern Med. 2007; 46:1365–71.
4. Tsushima K, Tanabe T, Yamamoto H, Koizumi T, Kawa S, Hamano H, et al. Pulmonary involvement of autoimmune pancreatitis. Eur J Clin Invest. 2009;39:714–22.
5. Fujinaga Y, Kadoya M, Kawa S, Hamano H, Ueda K, Momose M, et al. Characteristic findings in images of extra-pancreatic lesions associated with autoimmune pancreatitis. Eur J Radiol. 2010;76: 228–38.
6. Momose M, Kadoya M, Yano K, Miyasaka T, Fujinaga Y, Matsushita T, et al. Semiquantitative measurement of pulmonary hilar gallium-67 uptake using single photon emission computed tomography/computed tomography for the diagnosis of autoimmune pancreatitis. Jpn J Radiol. 2010;28:733–9.
7. Ishii S, Shishido F, Miyajima M, Sakuma K, Shigihara T, Kikuchi K. Whole-body gallium-67 scintigraphic findings in IgG4-related disease. Clin Nucl Med. 2011;36:542–5.
8. Aoki A, Sato K, Itabashi M, Takei T, Yoshida T, Arai J, et al. A case of Mikulicz's disease complicated with severe interstitial nephritis associated with IgG4. Clin Exp Nephrol. 2009;13:367–72.